Magnetostriction of Ruthenium-Substituted Yttrium Iron Garnet

P. Hansen
Philips Forschungslaboratorium Hamburg GmbH, 2 Hamburg 54, Germany
(Received 19 July 1972)

The contribution to the magnetostriction constants λ_{100} and λ_{111} of trivalent ruthenium ions on octahedral sites in yttrium iron garnet has been calculated in terms of the single-ion model. This leads to simple expressions of the temperature dependence of these quantities which is determined by the exchange field and the ratio of the trigonal field to the spin-orbit coupling. Using these atomic parameters which could be derived from the corresponding anisotropy data a satisfactory fit of the theory to experimental data could be achieved. The measurements of λ_{100} and λ_{111} have been carried out on single crystals of the composition $Y_3Fe_{5-x}Ru_xO_{12}$ by means of the resonant method in the temperature range of 4.2–500 K. The contribution of the Ru^{3+} ions turns out to be positive for both λ_{100} and λ_{111}.

I. INTRODUCTION

Transition-metal ions such as Fe^{2+}, Co^{2+}, Ru^{3+}, and Ir^{4+} in ferrites and garnets with an orbitally degenerate ground state in the cubic crystalline field generally give rise to pronounced effects in the anisotropy[1–10] and magnetostriction.[2,11–15] The anisotropy contributions can be interpreted in terms of the single-ion model[16,17] which takes into account the dependence on the direction of magnetization of the lowest energy levels which determine the magnetic behavior of these ions. This dependence is determined by the interactions which lift the degeneracy of the cubic ground state and the magnitude of the effect is mainly due to the relative magnitude of these interactions. The contribution to the magnetostriction is caused in addition by that increment of crystal field which depends on strain because it produces a strain dependence of the lowest energy levels. This involves the free energy to be a function of the direction of magnetization and the strain tensor. Up till now, the single-ion model has been applied to magnetostrictive effects[11–13] and a qualitative agreement between theory and experiment could be achieved only for Co^{2+}.[14]

For ruthenium in ferrites and garnets the dominant interactions are the local crystalline field, the spin-orbit coupling, and the exchange coupling which are responsible for the anisotropic behavior. Here the exchange interaction is the smallest term in contrast to Co^{2+}. In the case of low-spin Ru^{3+} in yttrium iron garnet (YIG) and gadolinium iron garnet (GdIG) the single-ion model accounts quantitatively for the observed anisotropy contributions using a level structure which is determined by these interactions. This quantitative agreement is believed to be mainly due to three reasons. First, no electron-transfer mechanism has been observed which would give rise to a reduction of the resistivity or the presence of field-induced effects as they have been observed for Fe^{2+}[1,2] or Co^{2+}.[4] Second, a very simple energy-level structure of low-spin Ru^{3+} ions is present showing three well-separated magnetic doublets. Third, the Ru^{3+} ions occupy (approximately) only octahedral sites in YIG and GdIG.

Owing to these facts the Ru^{3+} ions appear to be very promising concerning the study of their contribution $\Delta\lambda_{100}$ and $\Delta\lambda_{111}$ to magnetostriction because the total temperature dependence of $\Delta\lambda_{100}$ and $\Delta\lambda_{111}$ is expected to be essentially determined by the exchange field and the ratio of the local trigonal field to the spin-orbit coupling which are known from the corresponding anisotropy measurements.

In Sec. II we therefore calculate the temperature dependence of the contributions to the magnetostriction constants in terms of the single-ion model. In Sec. III the results are applied to ruthenium-doped YIG of the composition $Y_3Fe_{5-x}Ru_xO_{12}$ and the atomic parameters necessary to fit the experimental data are discussed. The measurements were carried out by means of the resonance technique at 9.25 GHz for $x=0$, 0.003, 0.009, and 0.021 in the temperature range of 4.2–500 K.

II. THEORY

The magnetostriction of cubic materials is usually described by the phenomenological expression of the magnetoelastic energy

$$E_{me} = b_0(\epsilon_{11}+\epsilon_{22}+\epsilon_{33}) + b_1(\alpha_1^2\epsilon_{11}+\alpha_2^2\epsilon_{22}+\alpha_3^2\epsilon_{33}) + 2b_2(\alpha_1\alpha_2\epsilon_{12}+\alpha_2\alpha_3\epsilon_{23}+\alpha_1\alpha_3\epsilon_{13})+\cdots ; \quad (1)$$

b_p, α_q, and ϵ_{pq} are the magnetoelastic constants, the direction cosines of the magnetization with respect to the cubic axis, and the components of the strain tensor, respectively (p, $q=1$, 2, 3, where 1, 2, and 3 refer to the cubic axis x, y, and z, respectively). Neglecting higher-order terms in Eq. (1) and introducing the functions

$$F_{pq}(\vec{\alpha}) = \frac{\partial E_{me}}{\partial \epsilon_{pq}} \quad , \tag{2}$$

we can relate the magnetostriction constants λ_{100} and λ_{111} to these function $F_{pq}(\vec{\alpha})$ evaluated in certain crystallographic directions of the magnetization by

$$\lambda_{100} = \frac{2[F_{33}(010) - F_{33}(001)]}{3(C_{11} - C_{12})} \quad ,$$
$$\lambda_{111} = \frac{-F_{12}(110)}{3C_{44}} \quad , \tag{3}$$

where C_{11}, C_{12}, and C_{44} are the elastic constants. We further make use of the relations

$$\lambda_{100} = -\tfrac{2}{3} b_1/(C_{11} - C_{12}) \quad ,$$
$$\lambda_{111} = -\tfrac{1}{3} b_2/C_{44} \quad . \tag{4}$$

To obtain the contribution of the Ru^{3+} ions to the magnetostriction constants we need to consider the free energy of these ions which is given by

$$\Delta F = -\frac{k_B T N}{n} \sum_{i=1}^{n} \ln Z_i \quad , \tag{5}$$

where k_B is Boltzman's constant, T is the temperature, N is the number of Ru^{3+} ions per cm^3, n is the number of magnetically inequivalent sites, and Z_i is the partition function at such a site. Furthermore, a statistical distribution of the ions on these sites has been assumed. Following Slonczewski[12] we expand Z_i according to Chester[18]:

$$Z_i = Z_{i0} + \sum_{m=1}^{\infty} Z_{im} \quad , \tag{6}$$

where the first terms are given by

$$Z_{i0} = \sum_j e^{-E_{ij}/k_B T} \quad ,$$
$$Z_{i1} = -\frac{1}{k_B T} \sum_j W_{jj} e^{-E_{ij}/k_B T} \quad , \tag{7}$$
$$Z_{i2} = -\frac{1}{k_B T} \sum_{j \neq k} \frac{W_{jk}^{(1)} W_{kj}^{(2)} e^{-E_{ij}/k_B T}}{E_{ij} - E_{ik}} \quad .$$

E_{i1} are eigenvalues of the unperturbed Hamiltonian and the matrix elements $W_{jk}^{(1)}$ and $W_{kj}^{(2)}$ are in general due to different perturbations of comparable order of magnitude. The summation in Eqs. (7) carries over all energy levels. To calculate these expressions we have to know the energy levels and the corresponding wave functions.

The ground state of the Ru^{3+} ions on octahedral sites in YIG is a low-spin t_{2g}^5 configuration due to the large cubic crystal field as shown in Fig. 1. This configuration is sixfold degenerated and transforms like the cubic representation T_{2g}. In the following we will neglect all effects which arise from interactions with higher energy levels associated with the $t_{2g}^4 e_g^1$ configuration since their influence is expected to be small due to the large energy separation. Then the sixfold degeneracy of the ${}^2T_{2g}$ state is removed by the single-ion Hamiltonian

$$\mathcal{H} = V_t(\vec{r}) - \xi \vec{L} \cdot \vec{S} + g\mu_B \vec{S} \cdot \vec{H}_{exch} + \delta V(\vec{r}, \vec{\epsilon}) \quad . \tag{8}$$

$V_t(\vec{r})$ is the local trigonal field. The second term represents the spin-orbit coupling, where λ has been replaced by the one-electron spin-orbit coupling parameter ξ which is simply related to λ by $\lambda = -\xi$ for a t_{2g}^5 configuration. The third term is the exchange energy which is treated in the molecular-field approximation and $\delta V(\vec{r}, \vec{\epsilon})$ represents the increment of the crystal-field energy depending on ϵ_{pq}. In garnets where we have a negative trigonal field the first three terms of Eq. (8) lead to a level structure of a low-spin t_{2g}^5 configuration according to Fig. 1. For $|v/\xi| \gtrsim 0.4$ [v is the one-electron trigonal field parameter and is defined as a matrix element of $V_t(\vec{r})$ with the wave functions given in Eqs. (12)] the energies can be explicitly expressed by[6,10]

$$E^{+}_{1/2}(i) = E_+ \pm \tfrac{1}{2} g\mu_B H_{exch} [(1 - 2c_+^2)^2 \cos^2\gamma_i + c_+^4 \sin^2\gamma_i]^{1/2} \quad ,$$
$$E^{0}_{1/2}(i) = E_0 \pm \tfrac{1}{2} g\mu_B H_{exch} \cos\gamma_i \quad ,$$
$$E^{-}_{1/2}(i) = E_- \pm \tfrac{1}{2} g\mu_B H_{exch} [(1 - 2c_+^2)^2 \cos^2\gamma_i + c_-^4 \sin^2\gamma_i]^{1/2} \quad , \tag{9}$$
$$E_0 = \xi(\tfrac{1}{2} + \tfrac{1}{3} v/\xi) \quad ,$$
$$E_\pm = -\tfrac{1}{2}\xi\{\tfrac{1}{2} + \tfrac{1}{3} v/\xi \pm [2 + (\tfrac{1}{2} - v/\xi)^2]^{1/2}\} \quad ,$$

and with wave functions

$$\Phi_1^{\pm}(i) = a_\pm(i)(\pm c_\pm t_3^+ + c_\mp t_1^-) e^{-i\delta_i/2} - b_\pm(i)(\mp c_\pm t_3^- + c_\mp t_2^+) e^{i\delta_i/2} \quad ,$$
$$\Phi_2^{\pm}(i) = b_\pm(i)(\pm c_\pm t_3^+ + c_\mp t_1^-) e^{-i\delta_i/2} + a_\pm(i)(\mp c_\pm t_3^- + c_\mp t_2^+) e^{i\delta_i/2} \quad , \tag{10}$$
$$\Phi^0_{1/2} = t^\pm_{1/2} \quad ,$$

where

$$c_+^2 = \frac{1}{2}\left(1 - \frac{\frac{1}{2} - v/\xi}{[2 + (\frac{1}{2} - v/\xi)^2]^{1/2}}\right) \quad ,$$
$$c_+^2 + c_-^2 = 1 \quad ,$$
$$a_+^2(i) = \frac{1}{2}\left(1 - \frac{(1 - 2c_+^2)\cos\gamma_i}{[(1 - 2c_+^2)^2 \cos^2\gamma_i + c_+^4 \sin^2\gamma_i]^{1/2}}\right) , \tag{11}$$
$$a_+^2(i) + b_+^2(i) = 1 \quad ,$$
$$a_-^2(i) = \frac{1}{2}\left(1 + \frac{(1 - 2c_+^2)\cos\gamma_i}{[(1 - 2c_+^2)^2 \cos^2\gamma_i + c_-^4 \sin^2\gamma_i]^{1/2}}\right) \quad ,$$
$$a_-^2(i) + b_-^2(i) = 1 \quad .$$

Here the $t_i^\pm$ are linear combinations of the d functions, which are quantized along the trigonal axis

and are defined by

$$t_1^{\pm}=\sqrt{\tfrac{2}{3}}\,\big|-2,\pm\tfrac{1}{2}\big\rangle+\sqrt{\tfrac{1}{3}}\,\big|1,\pm\tfrac{1}{2}\big\rangle\ ,$$
$$t_2^{\pm}=\sqrt{\tfrac{2}{3}}\,\big|2,\pm\tfrac{1}{2}\big\rangle-\sqrt{\tfrac{1}{3}}\,\big|-1,\pm\tfrac{1}{2}\big\rangle\ , \qquad (12)$$
$$t_3^{\pm}=\big|0,\pm\tfrac{1}{2}\big\rangle\ .$$

The numbers in the ket $|m_L,\ m_S\rangle$ are the quantum numbers of the z component of the orbital and spin momentum, respectively. γ_i and δ_i are the angles between the direction of magnetization and the quantization axis in the x_i, y_i, z_i frame, where the quantization axis z_i coincides with one of the four [111] directions.

Now $\delta V(\vec{r},\vec{\epsilon})$ and $\mathcal{H}'_{\rm exch}$ have to be treated as a perturbation, where $\mathcal{H}'_{\rm exch}$ is $\mathcal{H}_{\rm exch}$ less its submatrix in the doublet manifold. Then the matrix elements $W_{jk}^{(i)}$ occurring in Eqs. (7) can be calculated. However, with respect to the magnetostriction constants we need the quantities F_{ij}. From Eqs. (2) and (5)–(7) we obtain

$$\Delta F_{pq}=\frac{\partial\Delta F}{\partial\epsilon_{pq}}=-\frac{k_BTN}{n}\sum_{i=1}^{n}\frac{1}{Z_i}\frac{\partial Z_i}{\partial\epsilon_{pq}}\ , \qquad (13)$$

where ΔF_{pq} is the contribution due to the Ru^{3+} ions.

In the following we want to consider only matrix elements between the four energy levels $E^{+}_{1/2}$ and $E^{0}_{1/2}$, because $v/\xi<0$ for Ru^{3+} in YIG. $E^{-}_{1/2}$ only becomes important for positive values of v/ξ. This case applies for Ir^{4+} ions[6] and will not be considered here.

Further we want to restrict these calculations only to terms of first order in $\partial\delta V(\vec{r},\vec{\epsilon})/\partial\epsilon_{pq}$. Then we have to consider three terms which give rise to magnetostriction which can be expressed by

$$\frac{1}{Z_1}\frac{\partial Z_{i1}}{\partial\epsilon_{pq}}=-\frac{1}{k_BTZ_i}\sum_{l=1}^{2}\left(\langle\Phi_l^{+}(i)|\frac{\partial\delta V(\vec{r},\vec{\epsilon})}{\partial\epsilon_{pq}}|\Phi_l^{+}(i)\rangle\,e^{-E_l^{+}(i)/k_BT}+\langle\Phi_l^{0}|\frac{\partial\delta V(\vec{r},\vec{\epsilon})}{\partial\epsilon_{pq}}|\Phi_l^{0}\rangle\,e^{-E_l^{0}(i)/k_BT}\right)\ ,$$

$$\frac{1}{Z_i}\frac{\partial Z_{i2}}{\partial\epsilon_{pq}}=-\frac{1}{k_BTZ_i}\sum_{k,l=1}^{2}\left(\langle\Phi_l^{+}(i)|\mathcal{H}'_{\rm exch}|\Phi_k^{0}\rangle\langle\Phi_k^{0}|\frac{\partial\delta V(\vec{r},\vec{\epsilon})}{\partial\epsilon_{pq}}|\Phi_l^{+}(i)\rangle\frac{e^{-E_l^{+}(i)/k_BT}}{E_k^{0}(i)-E_l^{+}(i)}+\text{c. c.}\right)\ , \qquad (14)$$

$$\frac{1}{Z_i}\frac{\partial Z_{i3}}{\partial\epsilon_{pq}}=-\frac{1}{k_BTZ_i}\sum_{k,l,m=1}^{2}\left(\langle\Phi_l^{+}(i)|\mathcal{H}'_{\rm exch}|\Phi_k^{0}\rangle\langle\Phi_k^{0}|\mathcal{H}'_{\rm exch}|\Phi_m^{+}(i)\rangle\langle\Phi_m^{+}(i)|\frac{\partial\delta V(\vec{r},\vec{\epsilon})}{\partial\epsilon_{pq}}|\Phi_l^{+}(i)\rangle\times\frac{e^{-E_l^{+}(i)/k_BT}}{[E_l^{+}(i)-E_m^{+}(i)][E_k^{0}(i)-E_l^{+}(i)]}+\text{c. c.}\right),$$

where c. c. means complex conjugate and

$$Z_i=2\exp\left(-\frac{E_+}{k_BT}\right)\left[\cosh\left(\frac{E_1^{+}(i)-E_2^{+}(i)}{2k_BT}\right)+\exp\left(-\frac{E_0-E_+}{k_BT}\right)\cosh\left(\frac{E_1^{0}(i)-E_2^{0}(i)}{2k_BT}\right)\right].$$

To evaluate these sums constants $W_{pq}^{(i)}$ will be defined according to the relations

$$\langle t_1|\frac{\partial\delta V_i(\vec{r},\vec{\epsilon})}{\partial\epsilon_{pq}}|t_2\rangle=\langle t_2|\frac{\partial\delta V_i(\vec{r},\vec{\epsilon})}{\partial\epsilon_{pq}}|t_1\rangle=W_{pq}^{(i)}\ ,$$
$$\langle t_1|\frac{\partial\delta V_i(\vec{r},\vec{\epsilon})}{\partial\epsilon_{pq}}|t_3\rangle=-\langle t_2|\frac{\partial\delta V_i(\vec{r},\vec{\epsilon})}{\partial\epsilon_{pq}}|t_3\rangle=\eta_{pq}W_{pq}^{(i)}\ , \qquad (15)$$

where according to Eq. (3), pq equals to 12 or 33 and $\eta_{12}=-\frac{1}{2}$ and $\eta_{33}=1$. Here $\delta V_i(\vec{r},\vec{\epsilon})$ represents the crystal field in the x_i, y_i, z_i frame. The constants $W_{pq}^{(i)}$ are not independent. From the transformation properties of $\delta V_i(\vec{r},\vec{\epsilon})$ we find

$$W_{33}^{(i)}\equiv W_{33}\ ,$$
$$W_{12}^{(1)}=W_{12}^{(2)}=-W_{12}^{(3)}=-W_{12}^{(4)}\equiv W_{12}\ , \qquad (16)$$

where $\vec{z}_1\parallel[111]$, $\vec{z}_2\parallel[\bar{1}\bar{1}1]$, $\vec{z}_3\parallel[\bar{1}11]$, and $\vec{z}_4\parallel[1\bar{1}1]$. Here $\vec{z}_i$ denotes the unit vector along the z_i axis.

The still relatively complicated relations for $(1/Z_i)\partial Z_{il}/\partial\epsilon_{pq}$ suggest the introduction of the following abbreviations:

$$\Delta_t=E_0-E_+=\tfrac{1}{2}\xi\{\tfrac{3}{2}+v/\xi+[2+(\tfrac{1}{2}-v/\xi)^2]^{1/2}\}\ ,$$
$$\Delta_{\pm}^{(i)}=\tfrac{1}{2}g\mu_BH_{\rm exch}(\cos\gamma_i\pm\{c_+^4+[(1-2c_+^2)^2-c_+^4]\cos^2\gamma_i\}^{1/2})\ , \qquad (17)$$
$$R_{\pm}^{(i)}=\frac{1}{2}\,\frac{(1\pm\Delta_{\mp}^{(i)}/\Delta_t)\tanh[(\Delta_+^{(i)}-\Delta_-^{(i)})/2k_BT]}{1-(\Delta_{\mp}^{(i)}/\Delta_t)^2}$$
$$S_{\pm}^{(i)}=\frac{1}{2}\,\frac{\tanh[(\Delta_+^{(i)}-\Delta_-^{(i)})/2k_BT]\pm\Delta_{\mp}^{(i)}/\Delta_t}{1-(\Delta_{\mp}^{(i)}/\Delta_t)^2}\ .$$

With these quantities Eqs. (14) can be written in the form

$$\frac{1}{Z_i}\frac{\partial Z_{i1}}{\partial\epsilon_{pq}}=-\frac{2e^{-E_+/k_BT}}{k_BTZ_i}\left[W_{pq}^{+i}\cosh\left(\frac{\Delta_+^{(i)}-\Delta_-^{(i)}}{2k_BT}\right)-4\eta_{pq}W_{pq}^{(i)}a_+(i)b_+(i)c_+c_-\cos\delta_i\sinh\left(\frac{\Delta_+^{(i)}-\Delta_-^{(i)}}{2k_BT}\right)\right.$$

$$+ W_{pq}^{0i} e^{-\Delta_t/k_BT} \cosh\left(\frac{\Delta_+^{(i)} + \Delta_-^{(i)}}{2k_BT}\right)\Big] \ ,$$

$$\frac{1}{Z_i}\frac{\partial Z_{i2}}{\partial \epsilon_{pq}} = \frac{4W_{pq}^{(i)} g\mu_B H_e a_+(i) b_+(i) c_-^2 \sin\gamma_i}{\Delta_t k_B T} \frac{e^{-E_+/k_BT}\cosh[(\Delta_+^{(i)} - \Delta_-^{(i)})/2k_BT]}{Z_i}$$

$$\times\left((S_+^{(i)} + S_-^{(i)})\cos 2\delta_i + \frac{Hc_+\eta_{pq}}{a_+(i)b_+(i)}\left[a_+^2(i)R_+^{(i)} + b_+^2(i)R_-^{(i)}\right]\right) \ ,$$

$$\frac{1}{Z_i}\frac{\partial Z_{i3}}{\partial \epsilon_{pq}} = -\frac{\eta_{pq} W_{pq}^{(i)} (g\mu_B H_e)^2 a_+(i) b_+(i)[a_+^2(i) - b_+^2(i)] c_+ c_-^3 \sin^2\gamma_i \cos\delta_i}{\Delta_t(\Delta_+^{(i)} - \Delta_-^{(i)}) k_B T Z_i} e^{-E_+/k_BT}\cosh\left(\frac{\Delta_+^{(i)} - \Delta_-^{(i)}}{2k_BT}\right)(R_+^{(i)} - R_-^{(i)}) \ , \tag{18}$$

where

$$W_{pq}^{0i} = \langle t_1|\frac{\partial \delta V_i(\vec{r}, \vec{\epsilon})}{\partial \epsilon_{pq}}|t_1\rangle = \langle t_2|\frac{\partial \delta V_i(\vec{r}, \vec{\epsilon})}{\partial \epsilon_{pq}}|t_2\rangle \ ,$$

$$W_{pq}^{+i} = c_-^2 W_{pq}^{0i} + c_+^2\langle t_3|\frac{\partial \delta V_i(\vec{r}, \vec{\epsilon})}{\partial \epsilon_{pq}}|t_3\rangle \ .$$

These relations can be simplified considerably, because for temperatures below the Curie temperature of most of the garnets we have $k_BT/\Delta_t \lesssim 0.3$ and $(\Delta_\pm^{(i)}/\Delta_t)^2 \ll 1$,[8,9] assuming ξ of the order of 1000 cm^{-1}. $k_BT/\Delta_t \lesssim 0.3$ implies that in good approximation Z_i can be replaced by

$$Z_{i0} = 2e^{-E_+/k_BT}\cosh\left(\frac{\Delta_+^{(i)} - \Delta_-^{(i)}}{2k_BT}\right) \ .$$

Then, making use of the fact that $(\Delta_+^{(i)})^2 \ll \Delta_t^2$, we can expand these relations in powers of Δ_t^{-n}. With these approximations, especially for the expression $(1/Z_i)(\partial Z_{i1}/\partial \epsilon_{pq})$, only the second term contributes to the magnetostriction. We therefore obtain

$$\frac{1}{Z_{i0}}\frac{\partial Z_{i1}}{\partial \epsilon_{pq}} = -\frac{2W_{pq}^{(i)} a_+(i) b_+(i)}{k_BT}\sum_n Q_{in}^{(1)}\Delta_t^{-n} \ , \tag{19}$$

where the first coefficients are given by

$$Q_{i0}^{(1)} = -2\eta_{pq} c_+ c_- \tanh\left(\frac{\Delta_+^{(i)} - \Delta_-^{(i)}}{2k_BT}\right)\cos\delta_i \ ,$$

$$Q_{i1}^{(1)} = 0 \ , \tag{20}$$

$$Q_{i0}^{(2)} = 0 \ ,$$

$$Q_{i1}^{(2)} = -2g\mu_B H_e c_-^2 \sin\gamma_i\left[\tanh\left(\frac{\Delta_+^{(i)} - \Delta_-^{(i)}}{2k_BT}\right)\cos 2\delta_i + \frac{1}{2}\frac{c_+\eta_{pq}\cos\delta_i}{c_- a_+(i) b_+(i)}\right] \ ,$$

$$Q_{i0}^{(3)} = Q_{i1}^{(3)} = 0 \ .$$

The two lowest orders of the expansion (19) represented by the coefficients (20) turn out to be a good approximation for the case of Ru^{3+} in YIG. Then $\Delta\lambda_{100}$ and $\Delta\lambda_{111}$ can be expressed explicitly by simple relations. From Eqs. (3), (13), (16), (19), and (20) we obtain

$$\Delta\lambda_{100} = \frac{4}{3}\frac{NW_{33}G}{C_{11} - C_{12}}\left[\left(c_+^2 + \frac{E_e}{\Delta_t}G\right)\tanh\left(\frac{E_e}{k_BT}\right) + \frac{E_e}{\Delta_t}\right] \ ,$$

$$\Delta\lambda_{111} = \frac{1}{6}\frac{NW_{12}G^2E_e}{C_{44}\Delta_t}\left(\frac{3\tanh[E_e(1+\epsilon)^{1/2}/k_BT]}{(1+\epsilon)^{1/2}} + \frac{\tanh[E_e(1-\epsilon)^{1/2}/k_BT]}{(1-\epsilon)^{1/2}}\right) , \tag{21}$$

where

$$E_e = \frac{g\mu_B H_e[2c_+^4 + (1 - 2c_+^2)^2]^{1/2}}{2\sqrt{3}} \ ,$$

$$\epsilon = \frac{c_+^4 - (1 - 2c_+^2)^2}{2c_+^4 + (1 - 2c_+^2)^2} \ , \tag{22}$$

$$G = \frac{\sqrt{2}(c_+c_-)}{[2c_+^4 + (1 - 2c_+^2)^2]^{1/2}} \ .$$

For Ru^{3+} in YIG the exchange energy $g\mu_B H_e$ is of the order 500 cm^{-1} [8,9] and this should give rise to

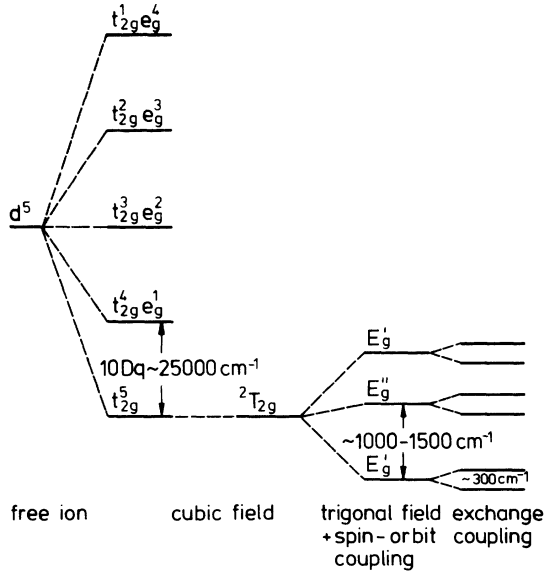

FIG. 1. Energy levels of Ru^{3+} with a low-spin d^5 configuration in YIG. The primed representations are of the double trigonal group. The energy differences are not to scale.

a slow temperature variation of $\Delta\lambda_{100}$ for $T < 300$ K as there H_e remains approximately constant for YIG. Above room temperature, however, the temperature dependence of the exchange field becomes important and will be dominant near the Curie temperature. The equation for $\Delta\lambda_{111}$ however, predicts a stronger temperature dependence.

III. EXPERIMENTS AND DISCUSSION

Single crystals of the composition $Y_3Fe_{5-x}Ru_xO_{12}$ have been investigated. They were grown from a $PbO-PbF_2-B_2O_3$ flux at about 1100 °C.[19,20] Very pure starting materials were used, i.e., especially the content of rare-earth impurities was of the order of 1 ppm. Effects on the magnetostriction due to the presence of other impurities such as Ca^{2+}, Si^{4+}, Pb^{2+}, Fe^{2+}, or F^-,[21] which are of the same magnitude for all crystals, can be neglected. The distribution of the ruthenium ions was found to be inhomogeneous. The concentration in the crystals varied at most by a factor of 2 on a distance of about 1 cm. This was the highest value found in a crystal among all batches. Therefore, it was necessary to determine the ruthenium content in the same single-crystal spheres where the magnetic measurements have been performed. This was possible by atomic-absorption measurements on the homogenized specimens after finishing the magnetostriction measurements. The accuracy in the determination of the concentration was increased with increasing Ru content. The results are summarized in Table I. The magnitude of the inhomogeneity in the single-crystal spheres could not be detected. However, this is not believed to be very important for the magnetic measurements since for these small concentrations no interaction between the ruthenium ions will occur. Measurements were performed on spheres of 0.7 mm in diameter applying the resonance method at 9.25 GHz according to Smith and Jones.[22,23] The spheres were oriented in the (110) plane with an accuracy of 0.5°. The temperature dependence has been studied in the range of 4.2–500 K. A compressional uniaxial stress τ in the [110] direction has been applied which causes a shift $\delta H_r[hkl]$ in the field for resonance $H_r[hkl]$ in the $[hkl]$ direction. The applied stress was between 10^7 and 10^8 dyn cm^{-2}. To calculate τ the effective area of the spheres was taken as $\frac{2}{3}\pi R^2$, where R is the radius. Then the measured values of λ_{100} and λ_{111} of pure YIG are in good agreement with those obtained by other methods.[24,25] From the shifts in the [001] and [110] directions the magnetostriction constants were deduced from the relations[22]

$$\lambda_{100} = -\tfrac{2}{3}(M_s/\tau)\delta H_r[001] ,$$

$$\lambda_{111} = -\frac{4}{9}\frac{M_s}{\tau}\left(1+\frac{1}{3}\frac{K_2}{M_s H_r[110]}\right)^{-1} \times\left[\left(1-\frac{2K_1-K_2}{4M_s H_r[110]}\right)\delta H_r[110] + \frac{1}{2}\left(1-\frac{2K_1}{M_s H_r[110]}\right)\delta H_r[001]\right] . \quad (23)$$

M_s, K_1, and K_2 are the saturation magnetization and the first and second anisotropy constant, respectively. The linear relationship between $\delta H_r[hkl]$ and τ could be verified in all cases. M_s has been measured with a vibrating sample magnetometer; however, no measurable deviations from the values of pure YIG occurred as has to be expected for such small substitutions. Thus, λ_{100} and λ_{111} could be calculated from Eqs. (23). For $0 \le x \le 0.02$ they were found to increase linearly with the ruthenium content as shown in Fig. 2 for $T = 295$ K in agreement with the values found by Krishnan *et al.*[15] (closed symbols). Deviations from this linearity have been observed for $x > 0.02$.[15] The temperature dependence of λ_{100} and λ_{111} is shown in Figs. 3(a) and 3(b) for samples Nos. 1–4. For sample No. 4 the measurements could only be carried out down to 200 °K because the anisotropy and the linewidth became too large for lower temperatures.

Both λ_{100} and λ_{111} are shifted to positive values with increasing ruthenium content. The contribution of the Ru^{3+} ions to λ_{100} turns out to be essentially constant over a wide range of temperatures while that to λ_{111} decreases with temperature. This was expected from the relations (21). The magnitude of $\Delta\lambda_{111}$ at 4.2 K is larger then that of $\Delta\lambda_{100}$. This indicates that the two-constant theory assumed in (1) and (23) will not strictly apply in this temperature range. Here the higher-order constants b_3, b_4, and b_5 may become important, similar to the description of the anisotropy.[6,9] This gives rise to a higher inaccuracy for the low-temperature values. However, we will not take into account this effect due to higher-order terms because at the present state, only λ_{100} and λ_{111} evaluated from Eqs. (23) are available. Further-

TABLE I. Composition of the measured single-crystal spheres.

Material	Composition	$x \pm 0.001$	N(cm^{-3})
1	$Y_3Fe_{5-x}Ru_xO_{12}$	0	0
2		0.003	1.27×10^{19}
3		0.009	3.80×10^{19}
4		0.021	8.86×10^{19}

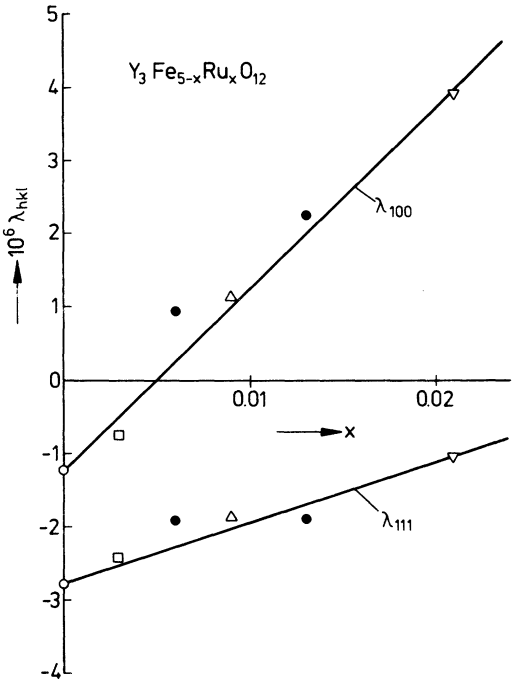

FIG. 2. Variation of the magnetostriction constants with the ruthenium concentration at $T=295$ K. The closed symbols are according to Krishnan *et al.* (Ref. 15).

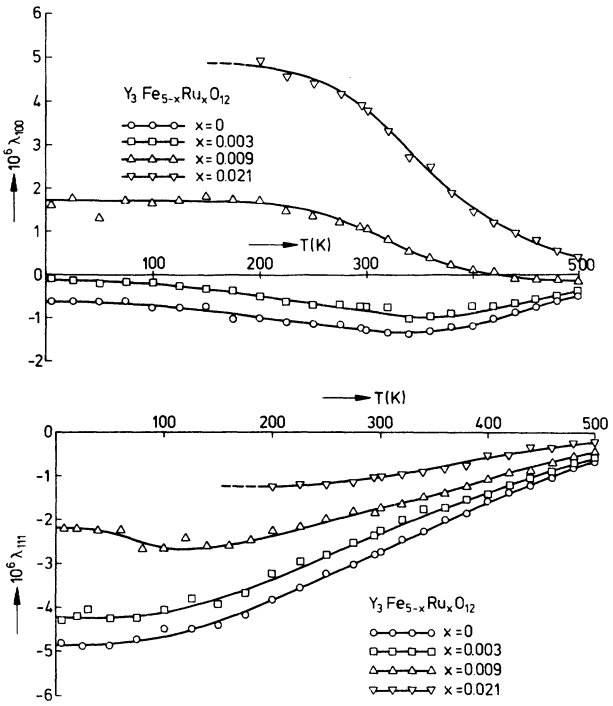

FIG. 3. Temperature dependence of (a) λ_{100} and (b) λ_{111} for ruthenium-doped garnet single crystals.

more, the deviation from linearity in the concentration occuring for $x>0.02$ indicates the presence of dipolar effects and interactions of the stress singularities of the Ru^{3+} ions and this may in addition affect the temperature dependence of sample No. 4.

To compare the experimental data with the theoretical results of Sec. II we, therefore, plot the contributions $\Delta\lambda_{hkl}=\lambda_{hkl}(x)-\lambda_{hkl}(0)$ vs temperature in Figs. 4(a) and 4(b) for sample No. 3. Sample No. 2 shows a much less pronounced effect due to the small Ru^{3+} concentration and appears less suitable to be compared with theory. To compute $\Delta\lambda_{hkl}$ from theory a number of parameters have to be known. The concentration $N=4.22\times10^{21}x$ is obtained from Table I. For the elastic constants

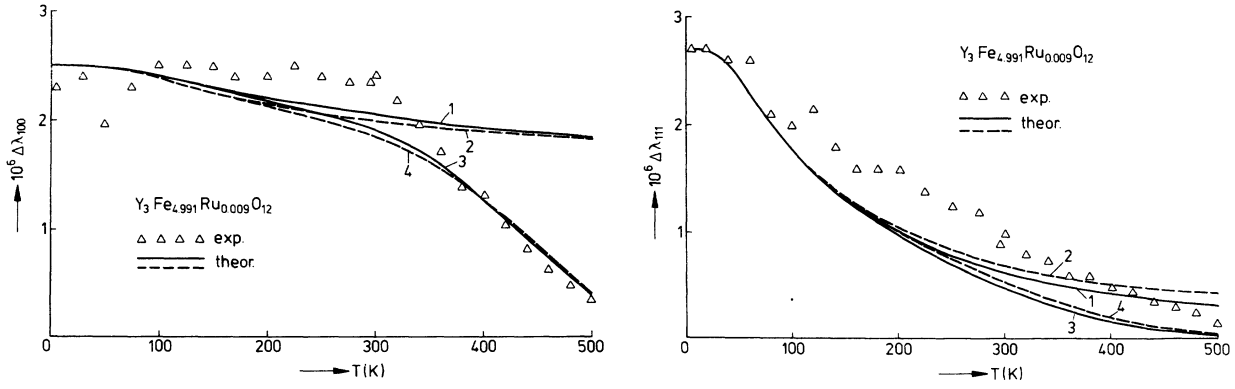

FIG. 4. Temperature dependence of (a) $\Delta\lambda_{100}=\lambda_{100}(x)-\lambda_{100}(0)$ and (b) $\Delta\lambda_{111}=\lambda_{111}(x)-\lambda_{111}(0)$ of sample No. 3. The theoretical curves are based on the values $v/\xi=-1$, $gH_e=1.2\times10^7$ Oe, $\xi=800$ cm^{-1}, $W_{33}=2100$ cm^{-1}, and $W_{12}=3100$ cm^{-1}. Curves 1 and 2 have been calculated with a temperature-independent exchange field and in the case of curves 3 and 4 a temperature variation of H_e according to the molecular-field theory (Refs. 27 and 28) has been introduced.

we use the values $C_{11} - C_{12} = 1.61 \times 10^{12}$ erg cm^{-3} and $C_{44} = 0.76 \times 10^{12}$ erg cm^{-3} for pure YIG at 296 K.[26] The one-electron spin-orbit coupling constant is expected to have a value between 700 and 1200 cm^{-1}; the value 800 cm^{-1} has been used. This choice is not important since the temperature dependence of $\Delta\lambda_{hkl}$ is not very sensitive in this range of ξ values. With these data the temperature dependence of $\Delta\lambda_{hkl}$ is completely determined by v/ξ and gH_e, and these quantities are known from the anisotropy to be of the order -1 and 10^7 Oe, respectively.[8,9] The remaining parameters W_{12} and W_{33} can now be deduced from the fit of the experimental values at 4.2 K. The best fit was obtained with $v/\xi = -1$, $gH_e = 1.2 \times 10^7$ Oe, $W_{33} = 2100$ cm^{-1}, and $W_{12} = 3100$ cm^{-1}.

The broken line in Figs. 4(a) and 4(b) represents the approximate theory according to Eqs. (21) and the solid line represents the results of the exact theory (without the approximations $\Delta_\pm^{(i)} \ll \Delta_t$ and $\Delta_t \gg k_B T$). Equations (21) are seen to be a good approximation. Only small deviations occur in the whole temperature range. The values $W_{12} = 3100$ cm^{-1} and $W_{33} = 2100$ cm^{-1} refer to the exact theory while those from the fit of Eqs. (21) are about 5% smaller. In both cases a temperature-independent exchange field has been assumed (curves 1 and 2). This is approximately correct up to room temperature. However, for higher temperatures this assumption is no longer justified due to the temperature variation of H_e. Especially the temperature dependence of $\Delta\lambda_{100}$ then is expected to be mainly governed by that of H_e and, therefore, should reflect essentially the temperature dependence of the magnetization of the tetrahedral sublattice. Thus, we have introduced a variation of H_e with T which is obtained from the fit of the saturation magnetization of YIG.[27,28] This leads to the theoretical curves 3 and 4 in Figs. 4(a) and 4(b).

Now a satisfactory fit to the experimental data in the whole temperature range is obtained and thus a consistent description of the anisotropy and magnetostriction by means of the single-ion model is possible using one set of atomic parameters. But there are some discrepancies between theory and experiment especially for $\Delta\lambda_{111}$. In this case the accuracy of the measurements become less good at low temperatures due to the large anisotropy where the [110] direction is the hard direction. Slightly higher values of $\Delta\lambda_{111}$ would lead to a much better fit of the temperature dependence.

However, there are still some other sources of error which may give rise to some changes in the values of the parameters used. As mentioned above we neglect the higher-order anisotropy and magnetostriction constants. Then, the strain in Eqs. (23) has been calculated using an effective area $\frac{2}{3}\pi R^2$, where the factor $\frac{2}{3}$ is only approximative. A change of this factor would directly affect W_{12} and W_{33}. Then, we have assumed all ruthenium ions to be exclusively in the trivalent state and to occupy only octahedral sites. Further effects of canting[29] or the presence of anisotropic exchange have been neglected.

IV. CONCLUSION

A strong change of the magnetostriction constants of yttrium iron garnet were caused by small amounts of Ru^{3+} ions. The contributions $\Delta\lambda_{100}$ and $\Delta\lambda_{111}$ were positive. Below 200 K, $\Delta\lambda_{100}$ turns out to be approximately constant while $\Delta\lambda_{111}$ strongly varies with T in the whole temperature range. This behavior could be well explained in terms of the single-ion model. The temperature variation of $\Delta\lambda_{100}$ and $\Delta\lambda_{111}$ is determined by the two lowest energy levels in good approximation. Below room temperature the higher levels effect the final result less than 10%. Thus, simple expressions for $\Delta\lambda_{100}$ and $\Delta\lambda_{111}$ could be derived for this case. The temperature dependence can essentially be described by two atomic parameters, i.e., the exchange field and the ratio of the trigonal field to the spin-orbit coupling. The knowledge of these parameters from the anisotropy contribution of Ru^{3+} leads to a satisfactory fit of the experimental data. Thus, a consistent explanation of the magnetic behavior with respect to anisotropy and magnetostriction has been achieved. Similar results are expected for other ions with a t_{2g}^5 configuration such as Ir^{4+} ($5d^5$) in garnets.

ACKNOWLEDGMENTS

The author wishes to thank Dr. W. Tolksdorf who grew and prepared the single-crystal specimens, Dr. J. Verweel for helpful discussions, J. Schuldt for performing the measurements, and Mrs. E. Haberkamp for the chemical analysis.

[1] T. S. Hartwick and J. Smit, J. Appl. Phys. **40**, 3995 (1969).
[2] P. Hansen, W. Tolksdorf, and J. Schuldt, J. Appl. Phys. **43**, 4740 (1972).
[3] J. C. Slonczewski, Phys. Rev. **110**, 1341 (1958).
[4] M. D. Sturge, E. M. Gyorgy, R. C. Le Craw, and J. P. Remeika, Phys. Rev. **180**, 413 (1969).
[5] R. Krishnan, Phys. Status Solidi A **1**, K17 (1970).
[6] P. Hansen, Philips Res. Repts. Suppl. **7**, 1 (1970).
[7] R. Krishnan, Phys. Status Solidi A **4**, K177 (1971).
[8] P. Hansen, Phys. Rev. B **3**, 862 (1971).
[9] P. Hansen, Phys. Status Solidi B **47**, 565 (1971).
[10] P. Hansen, Phys. Rev. B **5**, 3737 (1972).

[11]J. C. Slonczewski, J. Phys. Chem. Solids **15**, 335 (1960).
[12]J. C. Slonczewski, Phys. Rev. **122**, 1367 (1961).
[13]J. C. Slonczewski, J. Appl. Phys. **32**, 2535 (1961).
[14]R. D. Greenough and E. W. Lee, J. Phys. D **3**, 1995 (1970).
[15]R. Krishnan, V. Cagan, and M. Rivoire, AIP Conf. Proc. **5**, 704 (1971).
[16]K. Yosida and M. Tachiki, Prog. Theor. Phys. **17**, 331 (1957).
[17]W. P. Wolf, Phys. Rev. **108**, 1152 (1957).
[18]G. V. Chester, Phys. Rev. **93**, 606 (1954).
[19]W. Tolksdorf, J. Cryst. Growth **3/4**, 463 (1968).
[20]P. Hansen and W. Tolksdorf, J. Phys. (Paris) Suppl. **32**, C1-200 (1971).
[21]W. Tolksdorf and F. Welz, J. Cryst. Growth **13/14**, 566 (1972).
[22]A. B. Smith, Rev. Sci. Instrum. **39**, 378 (1968).
[23]A. B. Smith and R. V. Jones, J. Appl. Phys. **34**, 1283 (1963).
[24]E. DeLacheisserie and J. L. Dormann, Phys. Status Solidi **35**, 925 (1969).
[25]E. R. Callen, A. E. Clark, B. DeSavage, W. Coleman, and H. B. Callen, Phys. Rev. **130**, 1735 (1963).
[26]A. E. Clark and R. E. Strakna, J. Appl. Phys. **32**, 1172 (1961).
[27]E. E. Anderson, Phys. Rev. **134**, A1581 (1964).
[28]G. F. Dionne, J. Appl. Phys. **41**, 4874 (1970).
[29]P. Hansen, J. Appl. Phys. **43**, 650 (1972).

PHYSICAL REVIEW B VOLUME 8, NUMBER 1 1 JULY 1973

Effect of Exchange Interaction on the Low-Temperature Ordering of $GdCl_3$, Dysprosium Ethyl Sulfate, and Some Rare-Earth Hydroxides

Joshua Felsteiner
Physics Department, Technion-Israel Institute of Technology, Haifa, Israel

Sushil K. Misra
Physics Department, Sir George Williams University, Montreal 107, Canada

(Received 9 January, 1973)

The low-temperature ordered states of Gd^{+++} ions in gadolinium trichloride and hydroxide lattices, Dy^{+++} ions in dysprosium ethyl sulfate and hydroxide lattices, and Tb^{+++}, Ho^{+++}, Nd^{+++}, and Er^{+++} ions in their respective hydroxide lattices are investigated taking into account both the dipole-dipole and exchange interactions. The method used is essentially that of Luttinger and Tisza for dipole-dipole interaction, later generalized by Niemeyer to include exchange interaction. A linear dependence of the energy eigenvalues upon the exchange-interaction constants is found. For $GdCl_3$ and $Gd(OH)_3$, which are the only cases where the values of the exchange-interaction constants are experimentally known, ferromagnetic and antiferromagnetic orderings, respectively, corresponding to the lowest energy are predicted in agreement with the experimental observations. For $Nd(OH)_3$, where a ferromagnetic low-temperature ordering is predicted by the dipole-dipole interaction, an antiferromagnetic ordering may prevail if antiferromagnetic exchange interactions of suitable values are considered. This is in accordance with the observation of Wolf, Meissner, and Catanese. For the remaining cases, a limit for the next-nearest-neighbor exchange constant is obtained which will yield the ferromagnetic ordered states as observed experimentally.

I. INTRODUCTION

Recently many papers have appeared dealing with the prediction of ordered states at 0 °K, taking into account the magnetic dipole-dipole interaction between the constituent ions.[1-4] An exception is the work of Niemeyer,[1] which not only takes into account the dipole-dipole interaction but also includes the exchange interaction in his calculation for the case of cerium magnesium nitrate crystals. The method used for such calculations is essentially that developed by Luttinger and Tisza in 1946,[5] based on classical considerations. Niemeyer, on the other hand, has presented a quantum-mechanical treatment which yields the same prescription as the classical method. He also shows that the exchange interaction between nearest neighbors can be simultaneously taken into account. The present paper deals with the investigation of the low-temperature ordered states of Gd^{+++} ions in $GdCl_3$ and $Gd(OH)_3$ lattices, Dy^{+++} ions in dysprosium ethyl sulfate (DyES) and $Dy(OH)_3$ lattices, Tb^{+++} ions in $Tb(OH)_3$ lattice, Ho^{+++} ions in $Ho(OH)_3$ lattice, Nd^{+++} ions in $Nd(OH)_3$ lattice, and Er^{+++} ions in $Er(OH)_3$ lattice, under the effect of both magnetic dipole-dipole and exchange interactions. The rare-earth ions in all these crystals lie on lattices which are similar to hexagonal close-packed except that the c/a ratio is much smaller. The motivation for this investigation is provided by the finding that the dipole-dipole interaction alone does not predict the observed antiferromagnetic low-temperature ordering of $Nd(OH)_3$ and $Gd(OH)_3$.[3,4] The exchange interaction may then play an impor-